RSC Advances

ROYAL SOCIETY OF CHEMISTRY

www.rsc.org/advances

Journal Name

RSCPublishing

COMMUNICATION

Acid Induced Fluorinated Graphene Oxide

Cite this: DOI: 10.1039/x0xx00000x

Xuming Yang, Xinnan Jia, Xiaobo Ji*

Received 00th January 2012,
Accepted 00th January 2012

DOI: 10.1039/x0xx00000x

www.rsc.org/

White fluorinated graphene oxide was obtained from graphene oxide under hydrothermal conditions with the coexistence of nitric and hydrofluoric acid, and characterized with an atomic percentage of 21.5 for oxygen and 14.2 for fluorine, thus ensured of good dispersibility in water.

Graphene, monolayer carbon arranged in a hexagonal lattice, possesses many documented advantageous properties such as large specific surface area,[1] fast charged carrier intrinsic mobility[2] and excellent thermal conductivity,[3] and consequently shows great prospect for various applications including electronics, transparent conducting electrodes, energy conversion and storage devices and so on.[4-6] Chemical modification, an effective way to tailor properties of graphene, is one of the most active graphene research areas.[7] In comparison with graphene, graphene oxide (GO) has an improved dispersibility in aqueous or organic media, excellent reaction activity and defect-rich feature,[8] thus it is considered to be an excellent precursor for other graphene derivates and graphene-based composites.[9, 10]

Other than GO, fluorinated graphene (FG) has triggered a similar study enthusiasm.[11-14] It has been adopted in a range of applications such as a magnetically responsive drug carrier that can serve both as a magnetic resonance imaging (MRI) and photo-acoustic contrast agents,[15] super amphilphobic surfaces[16] and photonic devices[17]. The introduction of fluorine can remarkably reduce the electrical conductivity and opens up the band gap due to the transformation of sp^2 carbon to sp^3 carbon with the destruction of the highly delocalized conjugated system, thus turns graphene into special two-dimensional semiconductor. Additionally it has been reported that fluorinated graphene has a high nonlinear absorption and scatting with its optical limiting threshold reported to be an order of magnitude greater than just GO.[18]

Currently fluorinated graphene is produced mainly through liquid-phase or mechanical exfoliation of graphite fluoride[19, 20] as well as forced fluorination of graphene with F_2 or XeF_2 gas.[19, 21] The former always results to be multi-layer FG sheets, while the latter is quite dangerous and costly. To search for safe and facile synthetic methods, extensive attempts have been made with much moderate fluorinating reagents including hydrofluoric acid (HF) and fluorine-containing ionic liquid or organic compounds.[11, 22, 23] And HF, far less harsh than F_2 and XeF_2, is demonstrated to be a decent alternative in several reported works. [17, 24] Fluorinated reduced graphene oxide with tuneable degree of fluorination can be prepared via a hydrothermal treatment of graphene oxide (GO) with hydrofluoric acid at high temperature[17]; such an approach is a simultaneous process of fluorination and reduction that resulted in poor dispersibility of FG in common aqueous or nonaqueous media. If the reduction of GO was somehow restrained, oxygen-rich fluorinated graphene oxide (FGO) that owns the feature of GO would be obtained. To achieve this goal, conducting fluorination of GO in an oxidizing system might be a good choice. In this communication water-soluble FGO is managed to be prepared via an acid inducing approach which is schematically presented in Figure 1. Note that it is the first time that nitric acid is employed to help induce fluorination of GO. The detailed fluorinating procedure was described below.

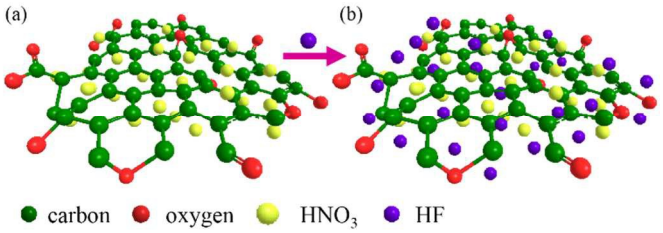

Figure 1. The schematic of acid inducing approach. Graphene oxide is hydrothermally treated with only HNO_3 (a) or HNO_3 and HF (b).

The fluorination of GO was accomplished through a hydrothermal treatment with the coexistence of HNO_3 and HF. It starts with the synthesis of GO from graphite which is then fluorinated to yield FGO. Specifically, 50 mg of GO prepared by Hummers method was dispersed in 40 mL of ultrapure water under ultrasonic, then centrifuged to

remove any insoluble substances. The supernatant was transferred into a 50 mL Teflon-lined stainless steel autoclave, then 5 mL of concentrated HNO_3 and 5 mL of HF was added while gently stirring. The autoclave was heated at 180℃ for 12 hours and naturally cooled to room temperature. The resultant solution was directly evaporated to dryness in water bath and the solids as prepared are fluorinated graphene oxide denoted as FGO (Figure 1b). Control sample denoted as NGO was synthesized following the same process except that 5 mL of ultrapure water was substituted for 5 mL of concentrated HNO_3 (Figure 1a).

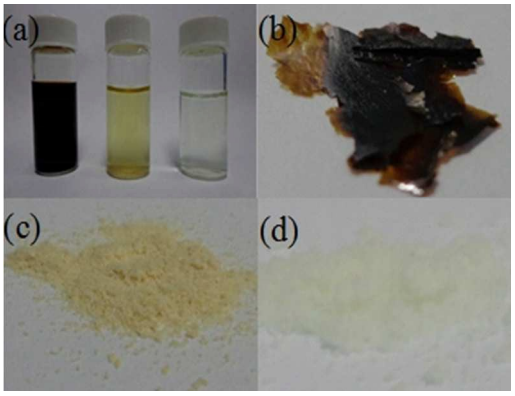

Figure 2. (a) Aqueous dispersions of GO, NGO and FGO (from right to left) at the concentration of 2 mg mL^{-1}; (b−d) solid GO, NGO and FGO.

The production of GO involving a Hummers method gives rise to rich oxygen groups like hydroxyl, epoxide and ketone groups, thus creates all-pervading active sites that can be connected or replaced with heteroatoms or even metal ions. With the comprehension of reported fluorinating effect of HF toward graphene oxide, we conduct it in the designed environment filled with oxidizing nitric acid, which would plausibly interact with GO and induce fluorine doping.

Figure 2 presents the visual demonstrations of fluorination where the colours of GO, NGO and FGO in a solid state or dispersed in water differ greatly from each other. The colour of GO dispersed in water is brown while that of NGO is yellow and FGO is nearly colourless/transparent. The pictures of solid GO, NGO and FGO are exhibited in Figure 2b−d. Brown GO sheets turn into a yellow NGO powder following hydrothermal treatment in HNO_3 (control sample where no HF is used), and strikingly, white FGO powder is obtained when HF is added. The strong difference in the observed colour indicates that HNO_3 and HF have played a vital role during the hydrothermal process and a remarkable composition change has occurred. The obvious change of colour of FGO material suggests a high degree of fluorination.[25, 26]

Transmission electron microscopy (HRTEM) was employed to explore the microstructure quality of the fabricated FGO and a typical transparent two-dimensional nanosheet-like structure is presented in Figure 3. But it was not perfect and smooth graphene sheet but covered by unordered wrinkles as observed. It is proposed to result from randomly distributed oxygen and fluorine groups that bonded with sp^3 carbon. Characterisation of the FGO was next sought using X−ray photoelectron spectroscopy (XPS).

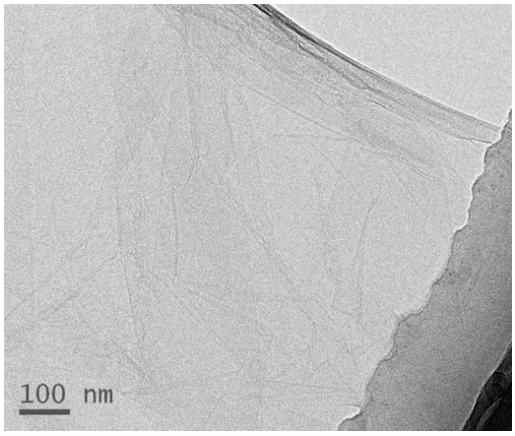

Figure 3. The TEM image of the synthesized FGO.

Figure 4a displays the XPS characterization of GO, NGO and FGO, and the quantified atomic percentages of carbon, oxygen and fluorine are presented in Table 1. NGO has a larger oxygen atomic percentage (39.2%) than GO (37.6%), and a trace of nitrogen was detected. The oxygen and fluorine atomic percentages of FGO are 21.5% and 14.2%, respectively demonstrating that a moderately fluorinated GO material has been fabricated. The reduction of the oxygen content is naturally attributed to the substitution of oxygen-containing groups by fluorine atoms. High resolution C1s spectra of GO, NGO and FGO are shown in Figure 4b−d, and the corresponding quantitative deconvolution results (operated in OriginLab OriginPro 8.5) are given in Table 2.

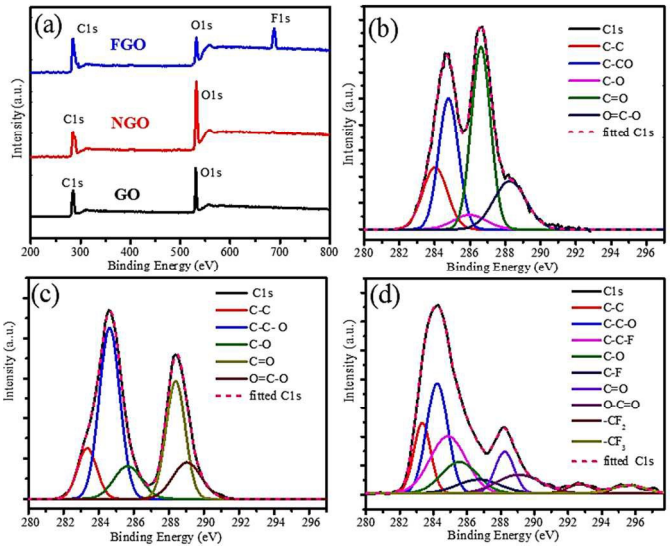

Figure 4. (a) XPS survey scan of GO, NGO and FGO; (b−d) high resolution C1s spectra of GO, NGO and FGO and their deconvolution results.

Through the comparison of carbon species in Table 1, we can observe that the proportions of C=O and O−C=O have slightly decreased, while the content of C−C−O vastly increased, which implies that hydroxyl or ether groups were generated as a result of the induction of nitric acid in the fabrication protocol. Interestingly, the shift of binding energy for C=O from 286.6 eV to 288.3 eV, leads the C1s spectrum of NGO to appear like a split doublet. The shift is ascribed to a different conjugation situation, which is obviously reflected in their

Fourier Transform Infrared (FTIR) spectra (Figure 5a) and ultraviolet-visible (UV−Vis) spectra (Figure 5b). The infrared absorption peak at 1625 cm^{-1} is stronger than at 1720 cm^{-1} for GO, and it is the reverse in case of NGO. The new absorption peak emerging at 280 nm in the UV−Vis spectrum of NGO is also thought to be caused by the different conjugation. The sharp peak at 1382 cm^{-1} in the FTIR spectrum of NGO corresponds to vibrations of carboxyl C−O stretching.

Table 1. Elemental compositions of GO, NGO and FGO

Element	Carbon	Oxygen	Fluorine
GO (%)	62.4	37.6	−
NGO (%)	60.6	39.2	−
FGO (%)	64.3	21.5	14.2

Table 2. Ascription content of carbon species of GO, NGO and FGO

Species	C−C	C−C−O	C−O	C=O	O−C=O	C−F[a]
GO (%)	15.8	26.8	4.96	36.3	16.2	–
NGO (%)	11.1	40.7	10.2	26.0	11.9	–
FGO (%)	12.6	24.9	12.0	8.41	8.71	11.4

a: The content of C−F in the table is given as the sum of C−F (6.23%), $C-F_2$ (2.36%) and $C-F_3$ (2.83%). Here the F/C ratio can be estimated to be 6.23% + 2×2.36% + 3×2.83% = 19.44%.

The high resolution C1s spectrum of FGO with a long tail at the high binding energy side via de-convolution shows the evidence of C−F being formed. As shown in Figure 4d, the experimental C1s spectrum is well fitted by nine Gaussian functions corresponding to nine sorts of carbon species and their ascription contents are quantitatively analysed by peak area normalization. In contrast to NGO, both the contents of C=O and O−C=O are reduced by the grafting of fluorine onto the graphene plane surface.

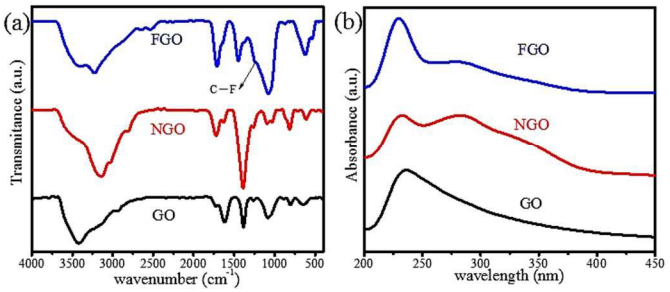

Figure 5. (a) FTIR spectra of GO, NGO and FGO; (b) UV−Vis spectra of GO, NGO and FGO.

The percentages of C−F (at 286.7 eV), $C-F_2$ (at 292.7 eV) and $C-F_3$ (at 295.7 eV) are 6.23%, 2.36% and 2.83%, respectively, based on which the fluorine to carbon atomic ratio ($R_{F/C}$) is estimated to be 0.194, that is slightly lower than the quantified $R_{F/C}$ (0.22) by XPS survey scan, suggesting a certain trance amount of fluorine not bonded but absorbed. C−F bonding is generally considered to be of two natures, namely, covalent bonding (sp^2 C−F) and semi−ionic bonding (sp^3 C−F). Stretching vibration absorption of covalent C−F at 1200 cm^{-1} can be clearly recognized for no interruption of C−O and it does not exist in the spectra of GO or NGO, nevertheless, semi−ionic C−F is difficult to be spotted due to the broad peak of C−O in the spectrum of FGO (Figure 5a).

High oxygen content of FGO identified via XPS is also reflected in the Fourier-transform infrared (FTIR) spectrum with characteristic peaks of various oxygen−containing groups such as 3220 cm^{-1} assigned to hydroxyl, 1720 cm^{-1} to carbonyl, 1382 cm^{-1} to carboxyl C−O, 1085 cm^{-1} to alkoxy C−O. The infrared absorption of FGO at the range of 1250−1000 cm^{-1} is much stronger than that of NGO, while the absorption at 28 nm in UV−Vis spectrum of FGO is much weaker than that observed in the UV−Vis spectrum of NGO (Figure 5b). These contrasts can be explained by the conjecture that fluorine was bonded to the active sites in graphene oxide plane where should have been oxidized by HNO_3.

When hydrothermally treated at relatively high temperatures (180 ℃), as commonly employed and reported in the literature,[27] GO is apt to precipitate into black powder. However, in this case with the use of HNO_3, GO dispersions turned into pellucid solutions with no precipitate. Neither was it when additional HF was in the aqueous system. On the contrary, the resultant fluorinated product is found to consist of a high oxygen content as expected, and no significant red shift of the max absorbance peak (around at 230 nm) was seen in the UV−Vis spectra (Figure 5b), which indicated that no serious reduction of GO has occurred. Here nitric acid is thought to serve as an oxidizing agent to sustain graphene oxide and help induce a moderate fluorination, which is quite different from literature attempts where usually the aim is to produce fluorinated reduced graphene oxide.

In the first work employing HF to induce the doping of fluorine into graphene oxide, fluorine is thought to be possibly bonded with carbon sites connected with oxygen atoms. Except the connected carbon, the neighbor carbon is also activated due to the strong electronegativity of oxygen, so it can also be the reaction site. That's to say introduction of fluorine and departure of oxygen may be separated. With the existence of oxidizing nitric acid, the fresh carbon sites created by the departure of oxygen groups (including carbon-oxygen groups) may be reoxidized. As the content of C=O decreased in NGO than in GO, and decreased further in FGO, while the content of C−O increased. It reasonably points to such an inference that carboxyl and carbonyl were replaced with hydroxyl, which explained how the nitric acid functioned. Alternatively, fluorine can be introduced at such sites with the coexistence of hydrofluoric acid. The processing is represented in Figure 6, and the sites are marked with different background colour.

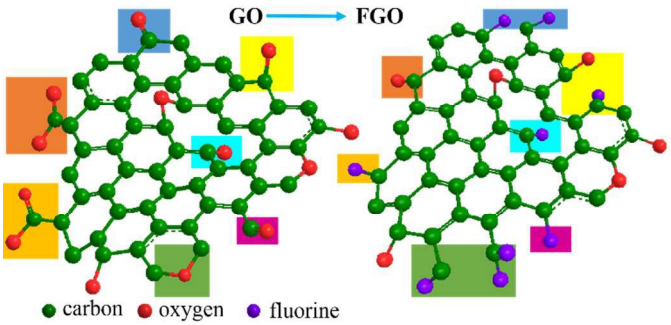

Figure 6. The schematic fluorination of GO into FGO.

Conclusions

In summary, we have prepared fluorinated graphene oxide via a hydrothermal route in a HF/HNO_3 mixed composition, which is characterized to be nonstoichiometric oxyfluorinated compound with an atomic percentage of 21.5 for oxygen and 14.2 for fluorine. The significant oxygen content makes it unique during documented fluorinated graphene. Additionally, it leads to good dispersibility in water, which may rouse more research interest of fluorinated graphene and fluorinated graphene based composites.

Financial support is from National Natural Science Foundation of China (21473258), Distinguished Young Scientists of Hunan Province (13JJ1004), and program for the New Century Excellent Talents in University (NCET-11-0513).

Notes and references

College of Chemistry and Chemical Engineering, Central South University, Changsha 410083, China. Tel: +86 731−88879616; Fax: +86 731− 88879616; E−mail: xji@csu.edu.cn

† Electronic Supplementary Information (ESI) available: a reported possible mechanism and detailed experimental procedures. See DOI: 10.1039/c000000x/

1. X. Li, W. Cai, J. An, S. Kim, J. Nah, D. Yang, R. Piner, A. Velamakanni, I. Jung and E. Tutuc, *Science*, 2009, **324**, 1312-1314.
2. K. I. Bolotin, K. Sikes, Z. Jiang, M. Klima, G. Fudenberg, J. Hone, P. Kim and H. Stormer, *Solid State Communications*, 2008, **146**, 351-355.
3. A. A. Balandin, S. Ghosh, W. Bao, I. Calizo, D. Teweldebrhan, F. Miao and C. N. Lau, *Nano letters*, 2008, **8**, 902-907.
4. V. Singh, D. Joung, L. Zhai, S. Das, S. I. Khondaker and S. Seal, *Progress in materials science*, 2011, **56**, 1178-1271.
5. M. J. Allen, V. C. Tung and R. B. Kaner, *Chemical reviews*, 2009, **110**, 132-145.
6. K. S. Novoselov, A. K. Geim, S. Morozov, D. Jiang, Y. Zhang, S. Dubonos, I. Grigorieva and A. Firsov, *Science*, 2004, **306**, 666-669.
7. J. Luo, J. Kim and J. Huang, *Accounts of chemical research*, 2013.
8. D. R. Dreyer, S. Park, C. W. Bielawski and R. S. Ruoff, *Chemical Society Reviews*, 2010, **39**, 228-240.
9. X. Huang, X. Qi, F. Boey and H. Zhang, *Chemical Society Reviews*, 2012, **41**, 666-686.
10. H. Bai, C. Li and G. Shi, *Advanced Materials*, 2011, **23**, 1089-1115.
11. J. Xiao, P. Meduri, H. Chen, Z. Wang, F. Gao, J. Hu, J. Feng, M. Hu, S. Dai, S. Brown, J. L. Adcock, Z. Deng, J. Liu, G. L. Graff, I. A. Aksay and J.-G. Zhang, *ChemSusChem*, 2014, **7**, 1295-1300.
12. R. J. Kashtiban, M. A. Dyson, R. R. Nair, R. Zan, S. L. Wong, Q. Ramasse, A. K. Geim, U. Bangert and J. Sloan, *Nat Commun*, 2014, **5**.
13. K.-I. Ho, C.-H. Huang, J.-H. Liao, W. Zhang, L.-J. Li, C.-S. Lai and C.-Y. Su, *Sci. Rep.*, 2014, **4**.
14. R. N. Gunasinghe, D. K. Samarakoon, A. B. Arampath, H. B. M. Shashikala, J. Vilus, J. H. Hall and X. Q. Wang, *Physical Chemistry Chemical Physics*, 2014, **16**, 18902-18906.
15. R. Romero-Aburto, T. N. Narayanan, Y. Nagaoka, T. Hasumura, T. M. Mitcham, T. Fukuda, P. J. Cox, R. R. Bouchard, T. Maekawa, D. S. Kumar, S. V. Torti, S. A. Mani and P. M. Ajayan, *Advanced Materials*, 2013, **25**, 5632-5637.
16. A. Mathkar, T. N. Narayanan, L. B. Alemany, P. Cox, P. Nguyen, G. Gao, P. Chang, R. Romero-Aburto, S. A. Mani and P. M. Ajayan, *Particle & Particle Systems Characterization*, 2013, **30**, 266-272.
17. Z. Wang, J. Wang, Z. Li, P. Gong, X. Liu, L. Zhang, J. Ren, H. Wang and S. Yang, *Carbon*, 2012, **50**, 5403-5410.
18. P. Chantharasupawong, R. Philip, N. T. Narayanan, P. M. Sudeep, A. Mathkar, P. M. Ajayan and J. Thomas, *The Journal of Physical Chemistry C*, 2012, **116**, 25955-25961.
19. R. Zbořil, F. Karlický, A. B. Bourlinos, T. A. Steriotis, A. K. Stubos, V. Georgakilas, K. Šafářová, D. Jančík, C. Trapalis and M. Otyepka, *Small*, 2010, **6**, 2885-2891.
20. K. Hou, P. Gong, J. Wang, Z. Yang, Z. Wang and S. Yang, *RSC Advances*, 2014.
21. J. T. Robinson, J. S. Burgess, C. E. Junkermeier, S. C. Badescu, T. L. Reinecke, F. K. Perkins, M. K. Zalalutdniov, J. W. Baldwin, J. C. Culbertson and P. E. Sheehan, *Nano letters*, 2010, **10**, 3001-3005.
22. F.-G. Zhao, G. Zhao, X.-H. Liu, C.-W. Ge, J.-T. Wang, B.-L. Li, Q.-G. Wang, W.-S. Li and Q.-Y. Chen, *Journal of Materials Chemistry A*, 2014, **2**, 8782-8789.
23. K. Samanta, S. Some, Y. Kim, Y. Yoon, M. Min, S. M. Lee, Y. Park and H. Lee, *Chem Commun*, 2013, **49**, 8991-8993.
24. L. Pu, Y. Ma, W. Zhang, H. Hu, Y. Zhou, Q. Wang and C. Pei, *RSC Advances*, 2013, **3**, 3881-3884.
25. H. Touhara and F. Okino, *Carbon*, 2000, **38**, 241-267.
26. X. Wang, Y. Dai, J. Gao, J. Huang, B. Li, C. Fan, J. Yang and X. Liu, *ACS Applied Materials & Interfaces*, 2013, **5**, 8294-8299.
27. Y. Zhou, Q. Bao, L. A. L. Tang, Y. Zhong and K. P. Loh, *Chemistry of Materials*, 2009, **21**, 2950-2956.

